

ALF: Adaptive Label Finetuning for Scene Graph Generation

Qisheng Chen

Center for Future Media, University
of Electronic Science and Technology
of China
Chengdu, China

Jianzhi Liu

Center for Future Media, University
of Electronic Science and Technology
of China
Chengdu, China

Xinyu Lyu

Center for Future Media, University
of Electronic Science and Technology
of China
Chengdu, China

Lianli Gao

Shenzhen Institute for Advanced
Study, UESTC
Shenzhen, China

Heng Tao Shen

Tongji University
Shanghai, China

Jingkuan Song

Tongji University
Shanghai, China

ABSTRACT

Scene Graph Generation (SGG) endeavors to predict the relationships between subjects and objects in a given image. Nevertheless, the long-tail distribution of relations often leads to biased prediction on coarse labels, presenting a substantial hurdle in SGG. To address this issue, researchers focus on unbiased SGG and introduce data transfer methods to transfer coarse-grained predicates into fine-grained ones across the entire dataset. However, these methods encounter two primary challenges: 1) They overlook the inherent context constraints imposed by subject-object pairs, leading to erroneous relations transfer. 2) Additional retraining process are required after the data transfer, which incurs substantial computational costs. To overcome these limitations, we introduce the first plug-and-play one-stage data transfer pipeline in SGG, termed *Adaptive Label Finetuning* (ALF), which eliminates the need for extra retraining sessions and meanwhile significantly enhance models' relation recognition capability across various SGG benchmark approaches. Specifically, ALF consists of two components: *Adaptive Label Construction* (ALC) and *Adaptive Iterative Learning* (AIL). By imposing Predicate-Context Constraints within relation space, ALC adaptively re-ranks and selects candidate relations in reference to model's predictive logits utilizing the Restriction-Based Judgment techniques, achieving robust relation transfer. Supervised with labels transferred by ALC, AIL iteratively finetunes the SGG models in an auto-regressive manner, which mitigates the substantial computational costs arising from the retraining process. Extensive experiments demonstrate that ALF achieves a 16% improvement in mR@100 compared to the typical SGG method Motif, with only a 6% increase in calculation costs compared to the state-of-the-art method IETrans. .

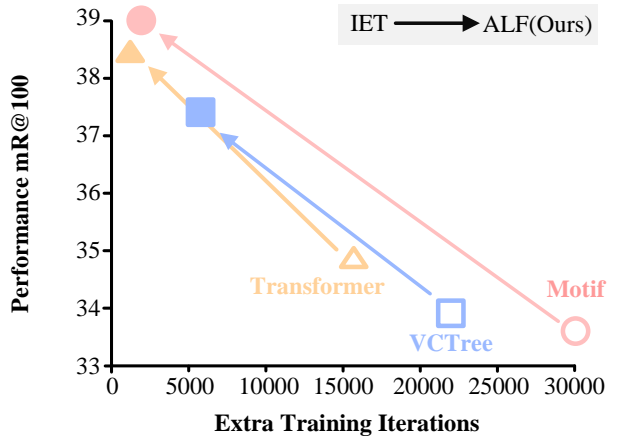


Figure 1: Comparison of extra training iterations (excluding the pretraining session) and performance between previous SOTA IETrans (marked as “IET”) and our Adaptive Label Finetuning (marked as “ALF”) with different baseline models on the VG50 dataset. As observed, our ALF achieves better performance with fewer extra training iterations than IETrans on three typical scene graph generation methods.

CCS CONCEPTS

• Computing methodologies → Artificial intelligence; Computer vision; Scene understanding;

KEYWORDS

Scene Graph Generation, Plug-and-Play, Data transfer, Adaptive Label Finetuning.

ACM Reference Format:

Qisheng Chen, Jianzhi Liu, Xinyu Lyu, Lianli Gao, Heng Tao Shen, and Jingkuan Song. 2024. ALF: Adaptive Label Finetuning for Scene Graph Generation. In *Proceedings of Make sure to enter the correct conference title from your rights confirmation email (ACM Multimedia 2024)*. ACM, New York, NY, USA, 10 pages. <https://doi.org/10.1145/nnnnnnnnnnnnnnnn>

1 INTRODUCTION

Scene Graph Generation (SGG) is a fundamental task for visual-language research, focusing on generating a semantic graph to

Permission to make digital or hard copies of all or part of this work for personal or classroom use is granted without fee provided that copies are not made or distributed for profit or commercial advantage and that copies bear this notice and the full citation on the first page. Copyrights for components of this work owned by others than ACM must be honored. Abstracting with credit is permitted. To copy otherwise, or republish, to post on servers or to redistribute to lists, requires prior specific permission and/or a fee. Request permissions from permissions@acm.org.

ACM Multimedia 2024, Oct. 28–Nov. 01, 2024, Melbourne, Australia

© 2024 Association for Computing Machinery.

ACM ISBN 978-x-xxxx-xxxx-x/YY/MM...\$15.00

<https://doi.org/10.1145/nnnnnnnnnnnnnnnn>

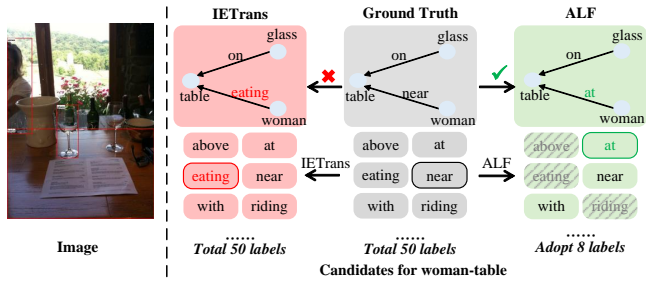


Figure 2: Example of IETrans (left) and our ALF (right). While IETrans disregards the constraints within subject-object pairs, chooses from all relations categories and sometimes leads to unsuitable label transfers (e.g., “eating” is inappropriate for the “woman-table” pair), it highlights that the predicates generated by IETrans may not always appropriately match the subject-object combination. Our method ALF adaptively narrows the selection of categories to 8 adopted labels through the restriction of subject-object pairs and avoids incorrect categories.

represent visual contents within a given image. This task serves as a pivotal bridge between computer vision and language, offering advantages for various visual comprehension tasks, including image captioning [1, 26, 45], cross-modal matching [14, 39, 41] and visual question answering [23, 31, 32, 43].

To address this issue, some researchers [16, 49] have identified the long-tailed distribution of predicates and semantic ambiguity within training datasets as the primary challenges. In datasets like Visual Genome [11], where over 90% of relation triplets contain fewer than 10 samples, hence SGG models face sub-optimal performance when predicting these underrepresented classes. For instance, current SGG methods [12, 42, 46, 50, 51] often predict coarse-grained relationship between subject-object pairs across numerous categories (e.g., “has”, “at”, and “in”) rather than fine-grained relationship (e.g., “belonging to”, “eating”, and “holding”), resulting in less informative predictions. Moreover, semantic ambiguity arises from predicates with similar semantics, such as “standing on”, “walking on”, and “parked on”, leading to ambiguous information due to their prevalence in the dataset. Consequently, due to these challenges, less common predicates like “standing on” and “walking on” are often misclassified as the more frequently occurring “on” by conventional SGG methods [3, 39–41, 45].

To address the aforementioned challenges, existing methods generally fall into two primary categories: learning-centric and data-centric debiasing approaches. Learning-centric approaches [6, 28, 29, 35] refine learning processes by introducing novel loss functions to enhance models' power on unbiased relation prediction and reduce semantic ambiguity across predicates sharing similar concepts. However, these approaches often suffer from inefficient training due to the complexity of the targeted learning algorithms. Conversely, data-centric approaches encompass techniques such as resampling [20] and data transfer [7, 16, 17, 49] to achieve a balanced data distribution across the entire dataset. Although resampling effectively refines labels with unclear semantics into more precise ones, it may reduce the dataset size, potentially impeding

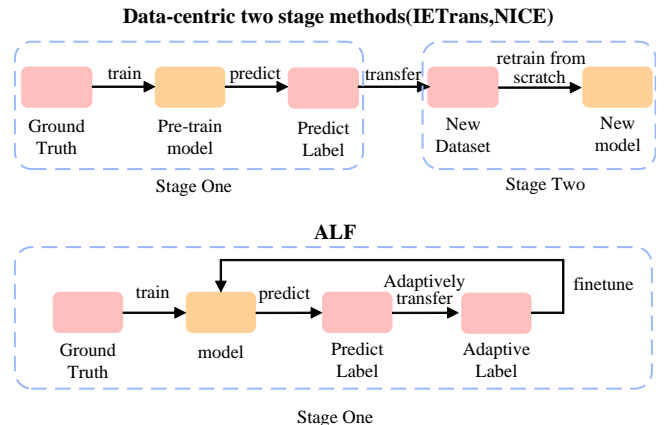


Figure 3: Comparison of learning paradigm between previous data-centric two-stage methods (up) and our ALF (down). Our ALF iteratively finetunes the pretrain model with adaptively generated labels, avoiding the huge training consumption associated with training from scratch.

effective feature learning. In contrast, data transfer methods generates fine-grained labels to alleviate label distribution imbalances, leveraging the entire sample set. However, current data transfer methods (e.g., IETrans [49]) overlook the contextual relevance between transferred labels and subject-object pairs, thereby failing to impose effective constraints in relation space and significantly reducing the accuracy of transferred labels. For instance, as depicted in Figure 2, IETrans wrongly transfers the predicate “near” to “eating” given subject-object pair as “woman-table”. Additionally, as shown in Figure 3, previous data-centric methods (IETrans [49], NICE [16] and ADTrans [17]) necessitate a two-stage training process due to dataset modifications. This process involves pre-training a model with original labels for data transfer, discarding the pre-trained models, and then initiating an additional training phase with the transferred data. Consequently, this two-stage training pipeline inevitably incurs significant training overhead.

To address these challenges, we introduce the first one-stage data transfer approach, namely Adaptive Label Finetuning (ALF), which can be seamlessly integrated with various baseline models in a plug-and-play fashion. In contrast to prior data transfer methods [16, 17, 49], ALF adaptively transfers data and meanwhile dynamically finetunes models during training, eliminating the need for extra retraining sessions. ALF comprises two key components: Adaptive Label Construction (ALC) and Adaptive Iterative Learning (AIL). ALC imposes subject-object constraints within relation space to re-rank and select appropriate predicates categories for data transfer, effectively averting the generation of implausible predicates. This process involves tallying and ranking the frequency of different relationships as the Predicate-Context Constraints knowledge, followed by employing a Restriction-Based Judgement mechanism to constrain data transfer based on these constraints and the model’s predictive logits during training. Since ALC transfer predicates in each training iteration based on the model’s prediction results, it produces more accurate transferred labels aligned with the model’s current learning status, enabling adaptive co-optimization

of both the model and data. Conversely, AIL iteratively finetunes the original model supervised by the transferred labels, bypassing the need to discard the pre-trained model and initiate training from scratch, as required in two-stage data transfer methods [16, 17, 49]. This approach facilitates more effective learning with improved performance.

Contribution: Our main contributions are summarized as follows:

- We propose the first plug-and-play one-stage data transfer approach, termed Adaptive Label Finetuning (ALF), which adaptively transfers data while dynamically finetuning models during training, thus obviating the necessity for additional retraining sessions.
- Adaptive Label Construction (ALC) constrains the relation space taking into account contextual relevance information, ensuring a robust data transfer process. Then, Adaptive Iterative Learning (AIL) iteratively finetunes SGG models with transferred data which are aligned with the model’s current learning status, facilitating an effective learning procedure.
- Extensive experiments are conducted on three benchmark models (Transformer, VCTree, and Motif), demonstrating that ALF consistently enhances performance compared to eight plug-in methods and six typical SGG models. Specifically, ALF achieves a 16% improvement in mR@100 over the typical SGG benchmark model Motif, with only a 6% increase in computational costs compared to the State-of-the-Art methods IETrans and NICE.

2 RELATED WORK

2.1 Scene Graph Generation

In recent years, numerous models [8, 12, 24, 25, 37, 42, 46, 50, 51] have emerged to tackle the task of scene graph generation from diverse perspectives. Additionally, [13] utilizes a graph generative approach and relational reasoning to generate scene graphs, thereby reducing training consumption. Moreover, [27] differentiates among hard-to-distinguish predicates for Scene Graph Generation task. [19] develop a transformerbased end-to-end framework that first generates the entity and predicate proposal set, followed by inferring directed edges to form the relation triplets. Further, [4] learns the model from simple to complex in a hierarchical learning pattern. Additionally, [48] exploit hypergraphs and propose hyper relationships to naturally and seamlessly integrate interaction and transitive inference. Moreover, [10] updates entity and relation features through an attention module for effective contextual reasoning, while [9] leverages spatial relations and object categories to obtain candidates for reasoning guidance. Furthermore, [22] design a knowledge distillation framework to transfer two types of external knowledge to the grounding module to help acquire high-quality “pseudo” ground truth for the subsequent SGG training process. [44] generate a more comprehensive scene graph representation based on panoptic segmentations rather than rigid bounding boxes. While these advancements have laid a solid foundation for scene graph generation, the long-tail distribution problem in scene graph datasets suggests that further improvements in dataset construction are necessary, as the enhancement of scene graph generation models alone is no longer the primary bottleneck. Researchers have

thus begun to focus on the dataset studies to address this biased issue.

2.2 Unbiased Scene Graph Generation

In addition to the aforementioned approaches, researchers [2, 5, 18, 30, 33, 34, 53] have explored diverse strategies to tackle the inherent distributional imbalance and bias issues in Scene Graph Generation (SGG) datasets. For instance, recent studies such as [49] have utilized pseudo-labeling techniques to generate augmented datasets, subsequently used for model training. By integrating additional data derived from pseudo-labeling, these models can learn to mitigate biased predictions, thereby enhancing their practical utility. [15] enrich the feature space of tail categories by augmenting both intrinsic and extrinsic features of the relation triplets. Moreover, [16] have proposed a method to reallocate predicate labels, prioritizing high-quality labels for noisy samples in SGG datasets. This label reassignment based on quality yields a cleaner dataset, facilitating more effective model training and diminishing the impact of noisy data on model performance. Furthermore, [7] have introduced a training strategy that incorporates both informative labels and original labels during model training. This approach enables models to learn complex reasoning by considering visual and textual constraints simultaneously, resulting in improved performance in handling biases inherent in SGG datasets. [21] integrate the predicate probability distribution into unbiased training loss. Building upon these endeavors, the current study aims to transfer biased predicate annotations into informative annotations to effectively address the distributional imbalance in SGG datasets. By leveraging informative annotations, the proposed approach aims to enhance model training and bolster the robustness of SGG models against bias-induced errors, thereby advancing the state-of-the-art in scene graph generation tasks.

3 METHOD

In this section, we begin by introducing some preliminary concepts in SGG and formulate essential models and parameters in Sec. 3.1. Subsequently, we present our Adaptive Label Construction and Adaptive Iterative Learning in Sec. 3.2 and Sec. 3.3. In particular, we only adopt the training data. The model and training loss function are consistent with the original model.

3.1 Preliminary

Scene Graph Generation (SGG) is a task that involves predicting the relationships $P = \{p_{(s_i, o_i)}\}$ between subject s_i and object o_i from image I . A scene graph corresponding to I has a set of objects $O = \{(b_i, c_i)\}$, where $b_i \in \mathbb{R}^4$ is an object bounding box, which are used to locate subjects and objects in image I ; c_i is an object class which contains subject s_i and object o_i . There are three sub-tasks in SGG: 1) **Predicate Classification** predicts the relationships P by given objects O and I . 2) **Scene Graph Classification** predicts not only relationships P but class label c_i based on a given bounding box b_i and its corresponding image I . 3) **Scene Graph Detection** only accepts image I as input and needs to predicts both objects O and their relationships P .

In order to solve the problem of long-tailed predicate distribution and semantic ambiguity, the prior data transfer method in SGG has

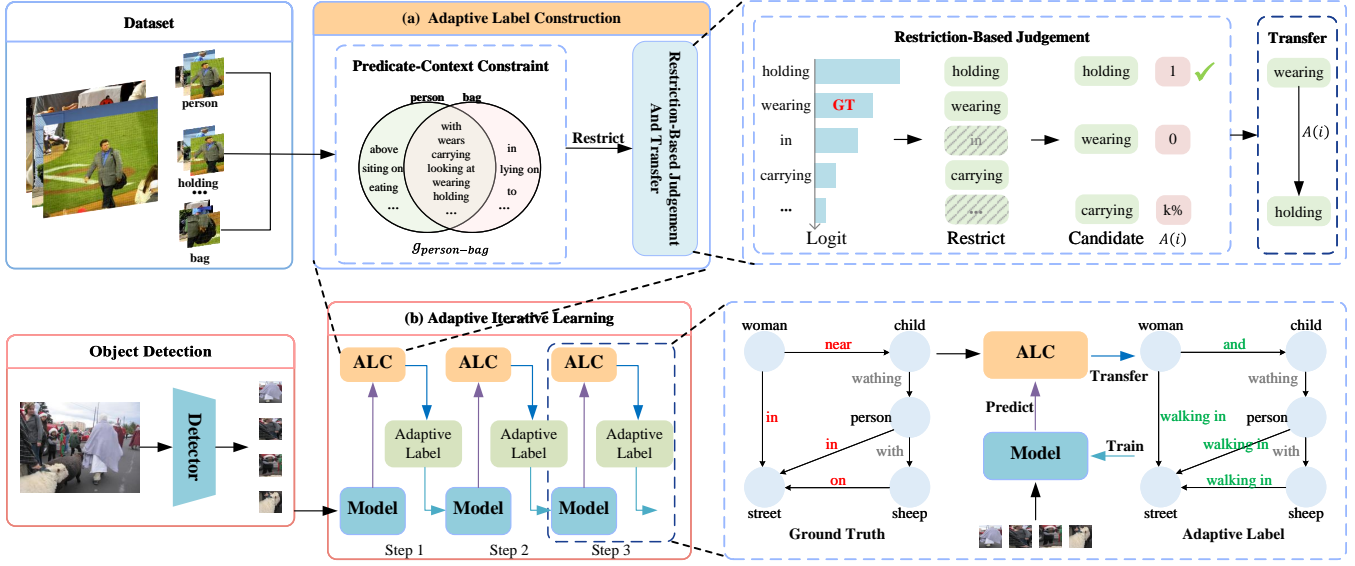


Figure 4: The overview of our ALF, which contains two composes: (a) Adaptive Label Construction to transfer data from coarse-grained predicate to fine-grained predicate. First, we use Predicate-Context Constraint to obtain a set of predicates associated with the subject-object pair from the dataset. Then, Restriction-Based Judgement uses Predicate-Context Constraint to restrict the predicate semantic space before transferring data. (b) Adaptive Iterative Learning iteratively finetunes the pretrained model with the enhanced labels generated by ALC in an autoregressive manner.

been proposed. Typical data transfer is a two-stage multi-class classification task. The first stage is that they train an SGG model \mathcal{M} normally and predict the original coarse-grained relation P_{ori} . The second stage is that they transfer the original coarse-grained relation P_{ori} to a new fine-grained relation P_{new} using a different strategy at the dataset level and retrain model \mathcal{M} from scratch to get a new model \mathcal{M}' . Those methods need huge retraining costs.

Our ALF first utilizes Adaptive Label Construction to restrict the predicate semantic space to avoid impossible predicates when transferring data. Then, Adaptive Iterative Learning finetunes the initial model with the enhanced labels in an autoregressive manner.

3.2 Adaptive Label Construction

The dataset's long-tailed distribution heavily suppresses rare predicates, overshadowed by frequently occurring ones during learning. This bias inclines the model towards predicting head predicates. However, head predicates, being more general, offer less informative predictions compared to non-head predicates. To rectify this, we aim to rebalance the predicate distribution by transforming head predicates into finer-grained non-head predicates, enhancing the value of the model's predictions.

Initially, the Predicate-Context Constraint acquires a set of predicates associated with the subject-object pair from the dataset by contextual analysis. Subsequently, to rectify the distribution imbalance across predicates, the Restriction-Based Judgment employs the Predicate-Context Constraint to confine the predicate space, obtaining candidate predicates, and then transfers the original labels P_{ori} to them.

For Scene Graph Generation (SGG), predicate selection hinges on contextual factors, which encompass the visual or semantic

attributes of the subjects s_i and objects o_i linked with the predicates P . For instance, as illustrated in Figure 2, when the object o is "table", it's evident that the predicate cannot be "eating". We posit that predicates associated with the same context, namely subject-object pairs, impose constraints based on context. Hence, we propose the Predicate-Context Constraint to extract context-based predicate constraints from all triplets in the training set. This constraint serves to confine the semantic space of predicates during data transfer, enabling the acquisition of transferred labels with finer granularity. **Predicate-Context Constraint:** We begin by counting the set of relations that appear for each entity when it serves as either the subject or object. Since both subjects and objects impose constraints on predicates, the intersection set of these relations is considered as all possible relations for this subject-object pair. In Figure 4a, the Predicate-Context Constraint structure is delineated. Herein, two sets are depicted: the green set denotes all relationships when the entity functions as a subject, while the pink set denotes the same when it serves as an object. Their intersection constitutes the set encompassing all instances of the subject-object pair's relationship in the dataset. For instance, both "with" and "carrying" can be utilized to describe relationships between "person" and "bag". Hence, these predicates P with the identical subject s and object o are amalgamated into the same set, i.e., $G = \{g_{s-o}\}$. The predicates P within the same set g_{s-o} are all viable options to delineate the relationship of a particular subject(s)-object(o) pair. This relationship is derived from existing matched pairs in the dataset, and the Restriction-Based Judgment technique is employed for screening and assessment. Consequently, context-based predicate constraints are established for all subject-object pairs.

Restriction-Based Judgement: Once the set of predicates associated with the subject-object pair is determined, the next step involves selecting the optimal candidate as the transferred label. To aid in this decision-making process, we introduce Restriction-Based Judgment, designed to identify the most suitable predicate from the candidate set g_{s-o} by considering both frequency and prediction priors.

To select the most suitable predicates from the candidate set g_{s-o} , we initially arrange the predicates in the training set in descending order of frequency of occurrence, selecting the top α as head predicates. This step ensures that only head predicates undergo transformation into non-head predicates, thereby balancing the predicate distribution. It's worth noting that, for subject-object pairs with ground truth predicate labels, any categories predicted as background are excluded. Subsequently, the model's predictions are sorted based on logits in descending order to derive P , from which the top few are selected to generate P_r . This process can be expressed as follows:

$$P_r = \{p_i \mid p_i \in P, i < l\} , \quad (1)$$

where $l = \text{len}(g_{s-o})$ denotes the size of the set g_{s-o} . And the index where the ground truth predicate label P_{gt} is located in P is denoted as l_{gt} .

Transfer: If a non-head predicate in P_r belongs to set g_{s-o} and surpasses the ground truth in prediction score, it is directly chosen as the transferred label, supplanting the original ground truth. This scenario arises when a non-head predicate, despite being typically overshadowed by head predicates, still outperforms the ground truth head predicate. This indicates the non-head predicate's exceptional suitability for the subject-object pair. Conversely, predicates with prediction scores lower than the ground truth are considered as candidates, and they are randomly replaced at a rate of $k\%$. The value of k is determined by the following formulation:

$$k = \frac{1}{i - l_{gt} + \beta} , \quad (2)$$

the β is a hyper-parameter. The farther away from the ground truth, the smaller the percentage of replacement. Therefore, the probability of transfer can be defined as:

$$P(A(i) = 1) = \begin{cases} 1, & i < l_{gt} \\ k\%, & l_{gt} < i < l \\ 0, & \text{else} \end{cases} , \quad (3)$$

where $A(i)$ indicates whether ground truth is replaced with the i -th predicate prediction. Note that, a triplet instance may need to be transferred to more than one relational triplet. To deal with the conflict, we choose the target predicate with the highest prediction score.

After obtaining the target predicate, we transfer ground truth to the adaptive label P_{new} based on $A(i)$. This transfer can be formulated as:

$$P_{new} = \{p_t A(t) + P_{gt} (1 - A(t)) \mid p_t \in P_r\} , \quad (4)$$

where P_{gt} denotes the ground truth predicate label and t denotes the index of target predicate.

3.3 Adaptive Iterative Learning

Prior methods involve pre-training a model for data transfer, followed by training it from scratch with the transferred data. Nonetheless, this approach has limitations. Firstly, the efficacy of transferred labels is contingent upon the quality of the pre-trained model; in other words, transferred labels are not optimized with the model and may not align with its current learning status. Secondly, discarding the pre-trained models and commencing training afresh with transferred data inevitably leads to significant training overhead.

To address these challenges, we introduce Adaptive Iterative Learning, aimed at generating labels aligned with the model's learning status while mitigating extensive training overhead associated with training from scratch. Illustrated in Figure 4b, our Adaptive Iterative Learning initially transfers a batch of data using Adaptive Label Construction. Subsequently, it trains the initial model with the newly generated enhanced labels in an autoregressive manner. As the model iteratively improves, the refined predictions feed back into the Adaptive Label Construction process (Eq. (1~4)) to generate more accurate and adaptive labels consistent with the model's learning status. ACL can be formulated as:

$$P_{new_i} = \text{ALC} \left(\text{Model}_{i-1}(s_i, o_i), P_{gt_i} \right) , \quad (5)$$

$$\text{Model}_i = \text{Train}(P_{new_i}) , \quad (6)$$

where $\text{Model}_i(s_i, o_i)$ denotes the predictions logits on (s_i, o_i) pair by the model that has been trained for i rounds using the transferred labels. This strategy mitigates the significant training overhead associated with training from scratch. Additionally, the refined labels, aligned with the model's learning status and increased accuracy, facilitate more efficient learning and improved performance. Importantly, during finetuning, we exclusively utilize non-head predicates, completely discarding the head predicate labels.

4 EXPERIMENT

To prove the efficiency of our proposed method ALC and AIL, we conduct extensive experiments on 8 plug-in baselines and 6 typical SGG models. In this section, we first introduce our experiment settings in 4.1. Second, we validate the effectiveness and generalization ability of our method in 4.2. Next, we present ablation studies to analyze the impacts of different factors in 4.3. Finally, we show some visualization results for additional efficiency proven in 4.5.

4.1 Experiment Setting

Baselines For our ALF is model-agnostic, following recent works [27, 49], we choose three SGG benchmark models as our baselines, including Motif [47], VCTree [36] and Transforme r[38] in SGG benchmark [35]. All models facilitate three typical scene graph generation tasks: predicate classification, scene graph classification, and scene graph detection. Experiments are conducted across these baselines for each task, with an average of five prior state-of-the-art models included in each baseline.

Datasets Following previous works [27, 35, 49, 52], we adopt widely used typical Visual Genome [11] split for scene graph generation. Visual Genome is the largest SGG dataset, which contains 101,174 images from MSCOCO with 50 predicate classes and 150 object classes.

Model	Predicate Classification			Scene Graph Classification			Scene Graph Detection			
	R@50 / 100	mR@50 / 100	F@50 / 100	R@50 / 100	mR@50 / 100	F@50 / 100	R@50 / 100	mR@50 / 100	F@50 / 100	
Specific	KERN	65.8 / 67.6	17.7 / 19.2	27.9 / 29.9	36.7 / 37.4	9.4 / 10.0	15.0 / 15.8	27.1 / 29.8	6.4 / 7.3	10.4 / 11.7
	GBNet	66.6 / 68.2	22.1 / 24.0	33.2 / 35.5	37.3 / 38.0	12.7 / 13.4	18.9 / 19.8	26.3 / 29.9	7.1 / 8.5	11.2 / 13.2
	BGNN	59.2 / 61.3	30.4 / 32.9	40.2 / 42.8	37.4 / 38.5	14.3 / 16.5	20.7 / 23.1	31.0 / 35.8	10.7 / 12.6	15.9 / 18.6
	DT2-ACBS	23.3 / 25.6	35.9 / 39.7	28.3 / 31.1	16.2 / 17.6	24.8 / 27.5	19.6 / 21.5	15.0 / 16.3	22.0 / 24.0	17.8 / 19.4
	PCPL	50.8 / 52.6	35.2 / 37.8	41.6 / 44.0	27.6 / 28.4	18.6 / 19.6	22.2 / 23.2	14.6 / 18.6	9.5 / 11.7	11.5 / 14.4
	PE-Net	64.9 / 67.2	31.5 / 33.8	42.4 / 44.9	39.4 / 40.7	17.8 / 18.9	24.5 / 25.8	30.7 / 35.2	12.4 / 14.5	17.7 / 20.5
Model-Agnostic	Motif	64.0 / 66.0	15.2 / 16.2	24.6 / 26.0	38.0 / 38.9	8.7 / 9.3	14.2 / 15.0	31.0 / 35.1	6.7 / 7.7	11.0 / 12.6
	+TDE	46.2 / 51.4	25.5 / 29.1	32.9 / 37.2	27.7 / 29.9	13.1 / 14.9	17.8 / 19.9	16.9 / 20.3	8.2 / 9.8	11.0 / 13.2
	+CogTree	35.6 / 36.8	26.4 / 29.0	30.3 / 32.4	21.6 / 22.2	14.9 / 16.1	17.6 / 18.7	20.0 / 22.1	10.4 / 11.8	13.7 / 15.4
	+EBM	- / -	18.0 / 19.5	- / -	- / -	10.2 / 11.0	- / -	- / -	7.7 / 9.3	- / -
	+DeC	- / -	35.7 / 38.9	- / -	- / -	18.4 / 19.1	- / -	- / -	13.2 / 15.6	- / -
	+DLFE	52.5 / 54.2	26.9 / 28.8	35.6 / 37.6	32.3 / 33.1	15.2 / 15.9	20.7 / 21.5	25.4 / 29.4	11.7 / 13.8	16.0 / 18.8
	+NICE	55.1 / 57.2	29.9 / 32.3	38.8 / 41.3	33.1 / 34.0	16.6 / 17.9	22.1 / 23.5	27.8 / 31.8	12.2 / 14.4	16.9 / 19.8
	+Inf	51.5 / 55.1	24.7 / 30.7	33.4 / 39.4	32.2 / 33.8	14.5 / 17.4	20.0 / 23.0	23.9 / 27.1	9.4 / 11.7	13.5 / 16.4
	+IETrans	54.7 / 56.7	30.9 / 33.6	39.5 / 42.2	32.5 / 33.4	16.8 / 17.9	22.2 / 23.3	26.4 / 30.6	12.4 / 14.9	16.9 / 20.0
	+ALF(Ours)	57.2 / 59.0	36.6 / 39.0	44.6 / 47.0	30.6 / 31.5	22.1 / 24.6	25.7 / 27.6	23.9 / 27.2	15.4 / 18.3	18.8 / 21.9
	VCTree	64.5 / 66.5	16.3 / 17.7	26.0 / 28.0	39.3 / 40.2	8.9 / 9.5	14.5 / 15.4	30.2 / 34.6	6.7 / 8.0	11.0 / 13.0
	+TDE	47.2 / 51.6	25.4 / 28.7	33.0 / 36.9	25.4 / 27.9	12.2 / 14.0	16.5 / 18.6	19.4 / 23.2	9.3 / 11.1	12.6 / 15.0
	+CogTree	44.0 / 45.4	27.6 / 29.7	33.9 / 35.9	30.9 / 31.7	18.8 / 19.9	23.4 / 24.5	18.2 / 20.4	10.4 / 12.1	13.2 / 15.2
	+EBM	- / -	18.2 / 19.7	- / -	- / -	12.5 / 13.5	- / -	- / -	7.7 / 9.1	- / -
	+DLFE	51.8 / 53.5	25.3 / 27.1	34.0 / 36.0	33.5 / 34.6	18.9 / 20.0	24.2 / 25.3	22.7 / 26.3	11.8 / 13.8	15.5 / 18.1
	+NICE	55.0 / 56.9	30.7 / 33.0	39.4 / 41.7	37.8 / 39.0	19.9 / 21.3	26.1 / 27.5	27.0 / 30.8	11.9 / 14.1	16.5 / 19.3
	+Inf	59.5 / 60.9	28.1 / 30.7	38.2 / 40.9	40.7 / 41.6	17.3 / 19.4	24.3 / 26.5	27.7 / 30.1	10.4 / 11.9	15.1 / 17.0
	+IETrans	53.0 / 55.0	30.3 / 33.9	38.6 / 41.9	32.9 / 33.8	16.5 / 18.1	22.0 / 23.6	25.4 / 29.3	11.5 / 14.0	15.8 / 18.9
	+ALF(Ours)	57.9 / 59.7	34.3 / 37.2	43.1 / 45.8	33.5 / 34.6	23.1 / 24.8	27.4 / 28.9	23.4 / 26.7	14.2 / 16.9	17.7 / 20.7
	Transformer	63.6 / 65.7	17.9 / 19.6	27.9 / 30.2	38.1 / 39.2	9.9 / 10.5	15.7 / 16.6	30.0 / 34.3	7.4 / 8.8	11.9 / 14.0
	+CogTree	38.4 / 39.7	28.4 / 31.0	32.7 / 34.8	22.9 / 23.4	15.7 / 16.7	18.6 / 19.5	19.5 / 21.7	11.1 / 12.7	14.1 / 16.0
	+IETrans	51.8 / 53.8	30.8 / 34.7	38.6 / 42.2	32.6 / 33.5	17.4 / 19.1	22.7 / 24.3	25.5 / 29.6	12.5 / 15.0	16.8 / 19.9
	+ALF(Ours)	53.3 / 55.2	35.9 / 38.4	42.9 / 45.3	29.0 / 30.0	21.3 / 22.6	24.6 / 25.8	22.8 / 26.2	14.8 / 17.5	17.9 / 21.0

Table 1: Comparison between existing methods and our method ALF on Visual Genome dataset.

Metrics We evaluate our methods on three sub-tasks in scene graph generation. Following previous works[27, 49], we use Recall@K (R@K) and mean Recall@K (mR@K) as metrics. However, different methods make different trade-offs between R@K and mR@K, making it difficult to make direct comparisons. Therefore, we further use a composite metric F@K, which is the harmonic average of R@K and mR@K, to jointly evaluate R@K and mR@K.

Implementation Details For the object detector, we utilize the Faster R-CNN pre-trained by [35] to detect objects in the image. In the training process, the parameters of the detector are frozen to reduce the computation cost. The batch size is configured to 12 except for Transformer, and we optimize all models employing cross-entropy loss with the SGD optimizer, initialized with a learning rate of 0.01. And for our ALF, the α is set to 25, and β is set to 2. For other training and inference settings, remain consistent with the original model.

4.2 Comparison with State of the Arts

We compare our method on results and finetune efficiency to other typical methods in this section.

4.2.1 Comparison of Results. To assess the efficacy of our proposed method, we compare it with 8 different models on three SGG baselines, i.e., Motif[47], VCTree[36] and Transformer[38]. As shown

Model	PredCls	
	ALC	AIL
		mR@50 / 100
		F@50 / 100
✓		15.2 / 16.2
		34.2 / 44.2
✓	✓	36.6 / 39.0
		44.6 / 47.0

Table 2: Ablation study on model components using Visual Genome dataset. ALC: Adaptive Label Construction; AIL: Adaptive Iterative Learning.

Method	Extra training iteration		
	Motif	VCTree	Transformer
NICE	30000	22000	16000
IETrans	30000	22000	16000
ALF	2000	6200	250

Table 3: Comparison of extra training iterations required for each benchmark model using different data transfer methods.

in Tab 1, the experiments are conducted across three different domains: Predicate Classification, Scene Graph Classification, and

Method	transfer ratio	mR@50 / 100	F@50 / 100
IETrans	47.63%	30.9 / 33.6	39.5 / 42.2
ALF	32.07%	36.6 / 39.0	44.6 / 47.0

Table 4: Transfer ratio and performance comparision between IETrans and our ALF on Motif.

α	5	15	25	35
R@100 \uparrow	59.99	56.74	58.97	58.08
mR@100 \uparrow	36.44	39.57	39.04	38.75
F@100 \uparrow	45.34	46.62	46.98	46.49

Table 5: Ablation study on hyper-parameter α using Visual Genome dataset.

Scene Graph Detection. The evaluation metrics include Recall (R), Mean Recall (mR), and F-score (F), measured at different thresholds (50 and 100). Under the Specific category, various models like KERN, GBNet, BGNN, DT2-ACBS, PCPL and PE-Net are evaluated. Notably, ALF (highlighted in gray) consistently demonstrates superior performance across these models.

In *Predicate Classification task*, ALF achieves Recall scores of 57.2/59.0 (at thresholds 50/100), Mean Recall of 36.6/39.0, and F-score of 44.6/47.0, indicating its robust capability in accurately identifying predicates within scenes. For *Scene Graph Classification task*, ALF maintains its effectiveness, with Recall scores of 30.6/31.5 (at 50/100), Mean Recall of 22.1/24.6, and F-score of 25.7/27.6. Furthermore, in *Scene Graph Detection task*, ALF continues to outperform, achieving Recall scores of 23.9/27.2 (at thresholds 50/100), Mean Recall of 15.4/18.3, and F-score of 18.8/21.9. These results underscore ALF’s proficiency in capturing the relationships between entities within images comprehensively. It is noteworthy that our results show lower performance compared to the baseline method in terms of R@50/100 metrics. This suggests an improvement in the long-tailed distribution of predictions after label balancing. Consequently, the model tends to prioritize predicting balanced data rather than solely focusing on the largest proportion of data as previously observed. Thus, a decrease in the model’s R@50/100 metrics is expected.

Overall, the consistent superiority of ALF across all three domains underscores its effectiveness in accurately identifying predicates and transferring data.

4.2.2 Comparison of Efficiency. To assess the efficiency of our methods, we compared the extra training iterations and transfer ratios with previous data transfer approaches (IETrans and NICE). Since it is hard to measure the extra training consumption of the re-label process within IETrans and NICE, we only calculate their extra training iterations during training from scratch process for efficiency comparison. As depicted in Table 3, ALF exhibits lower resource consumption. For instance, upon completing pre-training, IETrans and NICE on Motif, VCTree, and Transformer require re-training for 30,000, 22,000, and 16,000 iterations respectively,

β	1	2	3
R@100 \uparrow	58.26	58.97	59.12
mR@100 \uparrow	39.22	39.04	38.81
F@100 \uparrow	46.88	46.98	46.86

Table 6: Ablation study on hyper-parameter β using Visual Genome dataset.

whereas ALF requires only 2000, 6200, and 250 extra training iterations respectively. This discrepancy highlights the superior efficiency of our method. Moreover, ALF demonstrates more efficient data transfer. As illustrated in Table 4, when Motif serves as the benchmark model, our method only needs to transfer 32.07% of the data labels, compared to 47.63% for IETrans. This enhanced efficiency contributes to superior performance, underscoring the accuracy of our transfer method. Notably, we mitigate the weakening of the head predicate, elucidating why, as shown in Table 1, ALF outperforms IETrans on the R@100 metrics.

4.3 Ablation Studies

4.3.1 Impact of Hyper-Parameters α and β on ALF. To investigate the impact from different hyper-parameters on ALF, we conducted an ablation study on the number (α) of candidate sets (g_{s-o}) and the determining factors (β) of the selection rate ($k\%$). The selection of α is depicted in Figure 5. Given the dataset’s 50 categories, we experimented with values ranging from 5 to 35 in increments of 10 to determine the optimal α value. We observed that $\alpha = 25$ yields the best results for ALF. A large α may prompt the model to classify more predicates as head predicates, while a small α may overlook many head predicates requiring data transfer. Hence, we opted for a moderate value based on experimental findings. Similarly, the selection of β is illustrated in Figure 6. We varied β from 1 to 3 in steps of 1, with α fixed at 25. We determined that $\beta = 2$ is optimal for ALF, as it strikes an appropriate balance in the probability of selecting relations. Thus, we employed these settings across all experiments.

4.3.2 Effectiveness of the Devised Components in ALF. Our ALF contains two key components, including the ALC for guaranteeing a robust data transfer process, as well as the AIL for progressively generates enhanced labels and thereby iteratively finetuning models in a auto-regressive manner. We conduct component-wise investigation on the two components by incrementally adding one of them to the baseline method Motif on the PredCls task. From Tab 2, we observed that adding only Adaptive Label Construction (ALC) results in an 18% increase in mR@100 and an 18.2% increase in F@100 compared to the baseline model. Futhermore, the combination of ALC and AIL led to further performance enhancement, with mR@100 and F@100 reaching 39.0% and 47.0%, respectively. These results underscore the effectiveness of our ALF method.

4.4 Dataset Transfer Analysis

To examine the distribution of transferred labels, we present a visual comparison of data volumes across different relation class between the original and transferred datasets in Figure 5. The long-tail

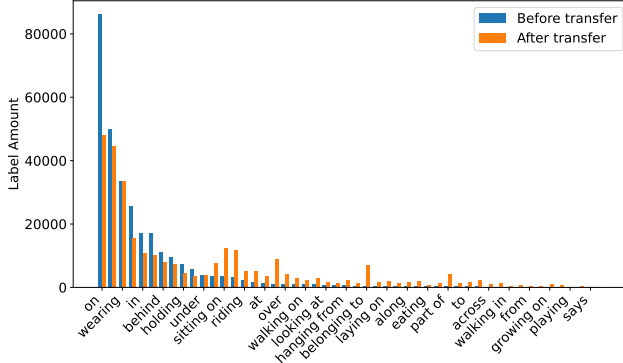


Figure 5: Comparison of data distribution across relations in Visual Genome datasets. The long-tail distribution is decreased from the original dataset (marked as blue) to AFL transferred dataset (marked as orange).

distribution noticeably decreases from the original dataset (indicated in blue) to the AFL transfer dataset (indicated in orange). Specifically, the prevalence of numerous labels, such as “on” is nearly halved compared to the original dataset. This illustrates the effectiveness of the AFL method in mitigating the long-tail distribution issue, which is a significant factor contributing to its efficacy. In Figure 6(a), we present visualised comparisons of transferred data from IETrans and our ALF, respectively, where IETrans incorrectly transfers “in front of” to “eating”, while ALF avoids this error.

4.5 Visualization Results

To visually demonstrate the efficacy of our proposed ALF, we compare scene graphs between the Motif baseline and Motif with ALF in Figure 6(b). It’s evident that Motif with ALF generates more fine-grained relationships compared to the Motif baseline, as exemplified by “plant-growing on-rock” versus “plant-near-rock”. Furthermore, ALF helps mitigate certain erroneous predictions, indicated by red labels such as “trunk-of-zebra”.

5 CONCLUSION

In this study, we introduce a plug-and-play method termed Adaptive Label Finetuning (ALF) aimed at refining coarse-grained predicate annotations into more informative ones at a finer granularity level, incurring minimal additional costs. ALF comprises two key components: Adaptive Label Construction (ALC) and Adaptive Iterative Learning (AIL). ALC enforces subject-object constraints within the relation space, effectively preventing the introduction of erroneous labels during the data transfer process. Subsequently, AIL progressively iteratively finetunes models supervised by data generated from ALC, thereby mitigating the substantial computational costs associated with the retraining process. Extensive experiments validate the effectiveness and efficiency of our proposed ALF method.

6 SOCIETAL IMPACTS AND LIMITATIONS

To elucidate the utility of our approach, we delineate the societal impacts and limitations in this supplementary section.

Societal Impacts: Scene Graph Generation, focusing on generating relation triplets within images, serves as a linchpin in various downstream tasks, including image captioning, cross-modal matching, and visual question answering. While recent advancements have seen large models tackling multiple tasks simultaneously, scene graph generation remains pivotal. Latest research underscores the utility of scene graphs as structured information to enhance the accuracy of large models. Leveraging scene graph generation can also address challenges such as model illusions associated with large-scale models.

Limitations: ALF seamlessly integrates into diverse baselines with minimal computational overhead, yielding impressive outcomes. However, existing Scene Graph Generation datasets are skewed towards common labels, lacking representation of rare labels. Consequently, when deploying SGG models for intricate proprietary tasks or alongside large-scale models in open domains, ALF may encounter challenges, particularly with complex verbs (e.g., “inquire”, “contain”, and “glance”) that pose comprehension and prediction difficulties initially. Addressing this limitation will be pivotal in future research endeavors aimed at augmenting the application of SGG in tandem with large-scale models.

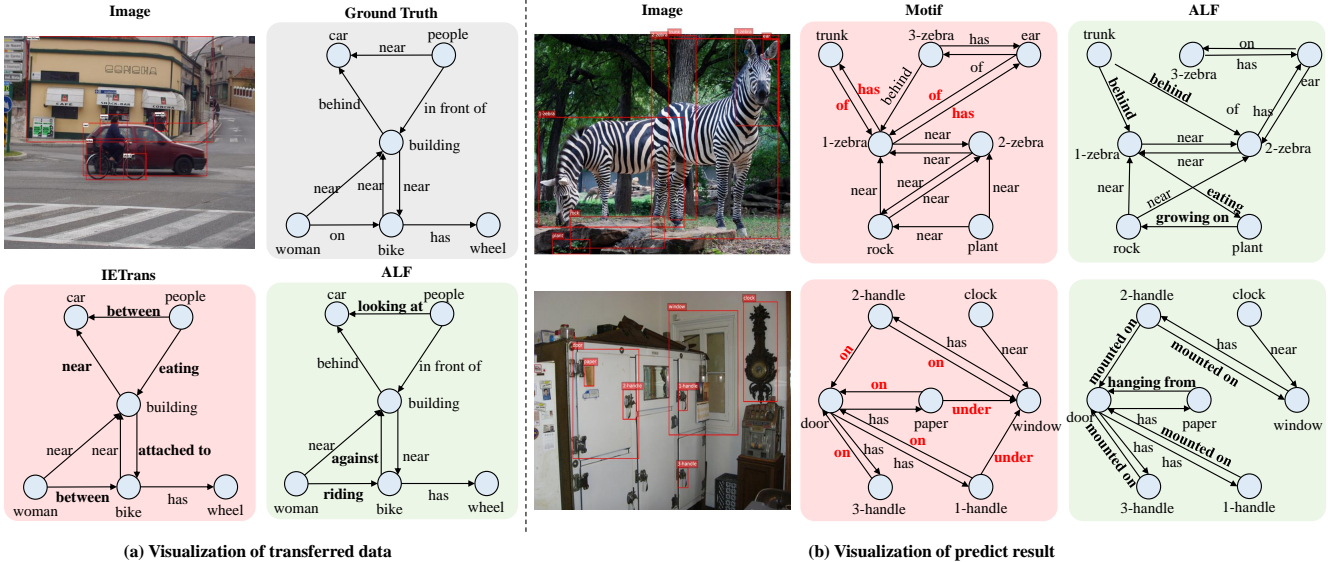


Figure 6: a) Visualization of transferred data of IETrans and ALF. b) Visualization result of the Motif baseline (in red) and Motif with our ALF (in green). The red label denotes unexpected relations prediction results.

REFERENCES

- [1] Yi Bin, Yujian Ding, Bo Peng, Liang Peng, Yang Yang, and Tat-Seng Chua. 2021. Entity slot filling for visual captioning. *IEEE Trans Circuits Syst Video Technol* (2021).
- [2] Bashirul Azam Biswas and Qiang Ji. 2023. Probabilistic debiasing of scene graphs. In *Proceedings of the IEEE/CVF Conference on Computer Vision and Pattern Recognition*. 10429–10438.
- [3] Min Chen, Xinyu Lyu, Yuyu Guo, Jingwei Liu, Lianli Gao, and Jingkuan Song. 2022. Multi-Scale Graph Attention Network for Scene Graph Generation. In *ICME*.
- [4] Youming Deng, Yansheng Li, Yongjun Zhang, Xiang Xiang, Jian Wang, Jingdong Chen, and Jiayi Ma. 2022. Hierarchical memory learning for fine-grained scene graph generation. In *CCV*.
- [5] Xingning Dong, Tian Gan, Xuemeng Song, Jianlong Wu, Yuan Cheng, and Liqiang Nie. 2022. Stacked hybrid-attention and group collaborative learning for unbiased scene graph generation. In *Proceedings of the IEEE/CVF Conference on Computer Vision and Pattern Recognition*. 19427–19436.
- [6] Lianli Gao, Xinyu Lyu, Yuyu Guo, Yuxuan Hu, Yuan-Fang Li, Lu Xu, Heng Tao Shen, and Jingkuan Song. 2023. Informative Scene Graph Generation via Debiasing. *arXiv preprint arXiv:2308.05286* (2023).
- [7] Arushi Goel, Basura Fernando, Frank Keller, and Hakan Bilen. 2022. Not all relations are equal: Mining informative labels for scene graph generation. In *CVPR*.
- [8] Tao He, Lianli Gao, Jingkuan Song, and Yuan-Fang Li. 2022. Towards open-vocabulary scene graph generation with prompt-based finetuning. In *European Conference on Computer Vision*. Springer, 56–73.
- [9] Tianlei Jin, Fangtai Guo, Qiwei Meng, Shiqiang Zhu, Xiangming Xi, Wen Wang, Zonghao Mu, and Wei Song. 2023. Fast contextual scene graph generation with unbiased context augmentation. In *Proceedings of the IEEE/CVF Conference on Computer Vision and Pattern Recognition*. 6302–6311.
- [10] Deunsol Jung, Sanghyun Kim, Won Hwa Kim, and Minsu Cho. 2023. Devil's on the edges: Selective quad attention for scene graph generation. In *Proceedings of the IEEE/CVF Conference on Computer Vision and Pattern Recognition*. 18664–18674.
- [11] Ranjay Krishna, Yuke Zhu, Oliver Groth, Justin Johnson, Kenji Hata, Joshua Kravitz, Stephanie Chen, Yannis Kalantidis, Li-Jia Li, David A Shamma, et al. 2017. Visual genome: Connecting language and vision using crowdsourced dense image annotations. *IJCV* (2017).
- [12] Sanjoy Kundu and Sathyaranarayanan N Aakur. 2022. Iterative scene graph generation with generative transformers. *arXiv preprint arXiv:2211.16636* (2022).
- [13] Sanjoy Kundu and Sathyaranarayanan N Aakur. 2023. IS-GGT: Iterative Scene Graph Generation With Generative Transformers. In *CVPR*.
- [14] Kunpeng Li, Yulun Zhang, Kai Li, Yuanyuan Li, and Yun Fu. 2022. Image-text embedding learning via visual and textual semantic reasoning. *TPAMI* (2022).
- [15] Compositional feature augmentation for unbiased scene graph generation. In *Proceedings of the IEEE/CVF International Conference on Computer Vision*. 21685–21695.
- [16] Lin Li, Long Chen, Yifeng Huang, Zhimeng Zhang, Songyang Zhang, and Jun Xiao. 2022. The devil is in the labels: Noisy label correction for robust scene graph generation. In *CVPR*.
- [17] Li Li, Wei Ji, Yiming Wu, Mengze Li, You Qin, Lina Wei, and Roger Zimmermann. 2023. Panoptic scene graph generation with semantics-prototype learning. *arXiv preprint arXiv:2307.15567* (2023).
- [18] Lin Li, Jun Xiao, Hanrong Shi, Wenxiao Wang, Jian Shao, An-An Liu, Yi Yang, and Long Chen. 2023. Label semantic knowledge distillation for unbiased scene graph generation. *IEEE Transactions on Circuits and Systems for Video Technology* (2023).
- [19] Rongjie Li, Songyang Zhang, and Xuming He. 2022. Sgtr: End-to-end scene graph generation with transformer. In *Proceedings of the IEEE/CVF conference on computer vision and pattern recognition*. 19486–19496.
- [20] Rongjie Li, Songyang Zhang, Bo Wan, and Xuming He. 2021. Bipartite graph network with adaptive message passing for unbiased scene graph generation. In *CVPR*.
- [21] Wei Li, Haiwei Zhang, Qijie Bai, Guoqing Zhao, Ning Jiang, and Xiaojie Yuan. 2022. Pndl: Predicate probability distribution based loss for unbiased scene graph generation. In *Proceedings of the IEEE/CVF Conference on Computer Vision and Pattern Recognition*. 19447–19456.
- [22] Xingchen Li, Long Chen, Wenbo Ma, Yi Yang, and Jun Xiao. 2022. Integrating object-aware and interaction-aware knowledge for weakly supervised scene graph generation. In *Proceedings of the 30th ACM International Conference on Multimedia*. 4204–4213.
- [23] Xiangpeng Li, Jingkuan Song, Lianli Gao, Xianglong Liu, Wenbing Huang, Xiangnan He, and Chuang Gan. 2019. Beyond rnns: Positional self-attention with co-attention for video question answering. In *AAAI*.
- [24] Xin Lin, Changxing Ding, Yibing Zhan, Zijian Li, and Dacheng Tao. 2022. Hl-net: Heterophily learning network for scene graph generation. In *proceedings of the IEEE/CVF conference on computer vision and pattern recognition*. 19476–19485.
- [25] Xin Lin, Changxing Ding, Jing Zhang, Yibing Zhan, and Dacheng Tao. 2022. Ru-net: Regularized unrolling network for scene graph generation. In *Proceedings of the IEEE/CVF Conference on Computer Vision and Pattern Recognition*. 19457–19466.
- [26] Hengyue Liu, Ning Yan, Masood S. Mortazavi, and Bir Bhanu. 2021. Fully Convolutional Scene Graph Generation. In *CVPR*.
- [27] Xinyu Lyu, Lianli Gao, Yuyu Guo, Zhou Zhao, Hao Huang, Heng Tao Shen, and Jingkuan Song. 2022. Fine-grained predicates learning for scene graph generation. In *CVPR*.

[28] Xinyu Lyu, Lianli Gao, Junlin Xie, Pengpeng Zeng, Yulu Tian, Jie Shao, and Heng Tao Shen. 2023. Generalized unbiased scene graph generation. *arXiv preprint arXiv:2308.04802* (2023).

[29] Xinyu Lyu, Lianli Gao, Pengpeng Zeng, Heng Tao Shen, and Jingkuan Song. 2023. Adaptive fine-grained predicates learning for scene graph generation. *TPAMI* (2023).

[30] Yukuan Min, Aming Wu, and Cheng Deng. 2023. Environment-Invariant Curriculum Relation Learning for Fine-Grained Scene Graph Generation. In *Proceedings of the IEEE/CVF International Conference on Computer Vision*. 13296–13307.

[31] Liang Peng, Yang Yang, Zheng Wang, Zi Huang, and Heng Tao Shen. 2020. Mra-net: Improving vqa via multi-modal relation attention network. *TPAMI* (2020).

[32] Jingkuan Song, Pengpeng Zeng, Lianli Gao, and Heng Tao Shen. 2022. From pixels to objects: Cubic visual attention for visual question answering. *arXiv preprint arXiv:2206.01923* (2022).

[33] Gopika Sudhakaran, Devendra Singh Dhami, Kristian Kersting, and Stefan Roth. 2023. Vision Relation Transformer for Unbiased Scene Graph Generation. In *Proceedings of the IEEE/CVF International Conference on Computer Vision*. 21882–21893.

[34] Shuzhou Sun, Shuaifeng Zhi, Qing Liao, Janne Heikkilä, and Li Liu. 2023. Unbiased scene graph generation via two-stage causal modeling. *IEEE Transactions on Pattern Analysis and Machine Intelligence* (2023).

[35] Kaihua Tang, Yulei Niu, Jianqiang Huang, Jiaxin Shi, and Hanwang Zhang. 2020. Unbiased scene graph generation from biased training. In *CVPR*.

[36] Kaihua Tang, Hanwang Zhang, Baoyuan Wu, Wenhan Luo, and Wei Liu. 2019. Learning to compose dynamic tree structures for visual contexts. In *CVPR*.

[37] Yao Teng and Limin Wang. 2022. Structured sparse r-cnn for direct scene graph generation. In *Proceedings of the IEEE/CVF Conference on Computer Vision and Pattern Recognition*. 19437–19446.

[38] Ashish Vaswani, Noam Shazeer, Niki Parmar, Jakob Uszkoreit, Llion Jones, Aidan N Gomez, Łukasz Kaiser, and Illia Polosukhin. 2017. Attention is all you need. *NIPS* (2017).

[39] Ni Wang, Zheng Wang, Xing Xu, Fumin Shen, Yang Yang, and Heng Tao Shen. 2021. Attention-based relation reasoning network for video-text retrieval. In *ICME*.

[40] Shuang Wang, Lianli Gao, Xinyu Lyu, Yuyu Guo, Pengpeng Zeng, and Jingkuan Song. 2022. Dynamic scene graph generation via temporal prior inference. In *ACM MM*.

[41] Zheng Wang, Zhenwei Gao, Xing Xu, Yadan Luo, Yang Yang, and Heng Tao Shen. 2022. Point to rectangle matching for image text retrieval. In *ICMM*.

[42] Zheng Wang, Xing Xu, Guoqing Wang, Yang Yang, and Heng Tao Shen. 2023. Quaternion relation embedding for scene graph generation. *IEEE Transactions on Multimedia* (2023).

[43] Zheng Wang, Jie Zhou, Jing Ma, Jingjing Li, Jiangbo Ai, and Yang Yang. 2020. Discovering attractive segments in the user-generated video streams. *Information Processing & Management* (2020).

[44] Jingkang Yang, Yi Zhe Ang, Zujin Guo, Kaiyang Zhou, Wayne Zhang, and Ziwei Liu. 2022. Panoptic scene graph generation. In *European Conference on Computer Vision*. Springer, 178–196.

[45] Xu Yang, Hanwang Zhang, and Jianfei Cai. 2020. Auto-encoding and distilling scene graphs for image captioning. *TPAMI* (2020).

[46] Qifan Yu, Juncheng Li, Yu Wu, Siliang Tang, Wei Ji, and Yueteng Zhuang. 2023. Visually-prompted language model for fine-grained scene graph generation in an open world. In *Proceedings of the IEEE/CVF International Conference on Computer Vision*. 21560–21571.

[47] Rowan Zellers, Mark Yatskar, Sam Thomson, and Yejin Choi. 2018. Neural motifs: Scene graph parsing with global context. In *CVPR*.

[48] Yibing Zhan, Zhi Chen, Jun Yu, BaoSheng Yu, Dacheng Tao, and Yong Luo. 2022. Hyper-relationship learning network for scene graph generation. *arXiv preprint arXiv:2202.07271* (2022).

[49] Ao Zhang, Yuan Yao, Qianyu Chen, Wei Ji, Zhiyuan Liu, Maosong Sun, and Tat-Seng Chua. 2022. Fine-grained scene graph generation with data transfer. In *ECCV*.

[50] Yong Zhang, Yingwei Pan, Ting Yao, Rui Huang, Tao Mei, and Chang-Wen Chen. 2023. Learning to generate language-supervised and open-vocabulary scene graph using pre-trained visual-semantic space. In *Proceedings of the IEEE/CVF Conference on Computer Vision and Pattern Recognition*. 2915–2924.

[51] Chengyang Zhao, Yikang Shen, Zhenfang Chen, Mingyu Ding, and Chuang Gan. 2023. Textpsg: Panoptic scene graph generation from textual descriptions. In *Proceedings of the IEEE/CVF International Conference on Computer Vision*. 2839–2850.

[52] Chaofan Zheng, Xinyu Lyu, Lianli Gao, Bo Dai, and Jingkuan Song. 2023. Prototype-based Embedding Network for Scene Graph Generation. In *CVPR*.

[53] Zijian Zhou, Miaoqing Shi, and Holger Caesar. 2023. Hilo: Exploiting high low frequency relations for unbiased panoptic scene graph generation. In *Proceedings of the IEEE/CVF International Conference on Computer Vision*. 21637–21648.